J.Serb.Chem.Soc. 68(4–5)349–361(2003)
JSCS – 3051

UDC 621.793:547.583.2:66.087
Original scientific paper

Roughness development in electrodeposited soft magnetic CoNiFe films in the presence of organic additives*

IBRO TABAKOVIĆ and STEVE RIEMER

Seagate Technology, One Disc Drive, Bloomington, MN 55435, USA

(Received 10 September 2002)

Abstract:The effects of three additives, sodium lauryl sulfate (NaLS), saccharin (Sacc), and NaLS + Sacc, on roughness development during the electrodeposition of CoNiFe films were investigated. The characterization of these films by atomic force microscopy shows that the electrodeposits produced from NaLS containing solution result in a rough surface. The role of NaLS surfactant is to change the interfacial tension and clean non-polar species like hydrogen bubbles from the surface. In Sacc containing solution, the evolution of a smooth surface is controlled by adsorbed Sacc molecule at the interface. The kinetic roughening of these deposits was investigated by dynamic scaling analysis. It was demonstrated that the roughness of CoNiFe films, obtained in the presence of NaLS + Sacc additives, was also dependent on current density, roughness of substrate, and the temperature of plating bath.

Keywords: soft magnetic CoNiFe films, morphology, roughness, saccharin, sodium lauryl sulfate, dynamic scaling analysis.

INTRODUCTION

Soft magnetic films with high magnetic moment (B_s), low coercivity (H_c), high permeability (μ), and uniaxial anisotropy (H_k) are essential for read and write heads in high-density magnetic recording. Since the coercivity of media is a measure of the field required to reverse the magnetic orientation of a bit, the recording head must generate a higher magnetic field to write effectively on the high coercivity media. Electrochemically prepared high magnetic moment (HMM) materials offer advantages such as higher rate of deposition, easier control of small features, and lower cost of processing when compared to sputtered films.[1] Efforts to find materials with higher B_s value than conventional alloys, *i.e.*, 1.0T $Ni_{80}Fe_{20}$ (Permalloy) and 1.6T $Ni_{45}Fe_{55}$, typically involve alloying them with Co. Recently soft CoNiFe alloys with $B_s = 1.8–2.1$T and $H_c < 2.0$ Oe were developed.[2–5]

The interfacial smoothness and planarity of electrodeposited magnetic layers are important for the processability and performance of magnetic heads. Organic additives are often used in electrodeposition of metals to moderate growth rates and to obtain smooth

* Dedicated to Professor Miroslav J. Gašić on the occasion of his 70th birthday.

films. Saccharin (Sacc) and sodium lauryl sulfate (NaLS) have been used for more than two decades in the industrial production of NiFe alloys and they are used in the preparation of CoNiFe alloys as well.[2–5] It has been reported that Sacc reduces the tensile stress and coercivity of CoNiFe[5] and NiFe[6] materials. Although it is generally known that the presence of Sacc in the plating bath reduces roughness of NiFe and CoNiFe films, there has been no systematic study of the influence of Sacc and NaLS additives on deposit surface morphology. The effects of Sacc on the texture[7–9] and roughness[10] of electrodeposited Ni films were reported.

The aim of the present work is to understand the specific role of the Sacc and NaLS additives in roughness development during the electrodeposition of CoNiFe films. The influence of parameters such as the thickness of deposited films, presence of additives in solution, current density, temperature of plating bath and cathode substrate on morphology of CoNiFe films is presented. Scanning electron microscope (SEM) and atomic force microscope (AFM) were used to examine the morphology of the electrodeposited surfaces. Kinetic roughening of CoNiFe deposits was investigated by dynamic scaling analysis. A number of studies have shown the feasibility of AFM and SEM techniques to study the kinetic roughening of thin films obtained by chemical vapor deposition,[11] physical vapor deposition,[12] molecular beam epitaxy,[13] and copper electrodeposition.[14–18]

EXPERIMENTAL

The electrodeposition of soft magnetic CoNiFe films was carried out on sputtered alumina wafers (6 in round) that each had a 1000 Å seed layer of sputtered Permalloy ($Ni_{83}Fe_{17}$). The CoNiFe films were electrodeposited using a chloride plating bath as described in the previous paper,[5] containing Sacc (0.6 g/l), NaLS (0.1 g/l) or Sacc + NaLS additives while keeping the concentrations of Co^{2+}, Ni^{2+}, and Fe^{2+} constant at pH of 2.8. The temperature was maintained at 23 ºC. A low current density (3 mA/cm^2) was used in order to attain a low growth rate (0.08 μm/min). Electrodeposition was carried out in a paddle cell (0.66 cycles/s) equipped with a filtered recirculation system and pH and temperature control. Uniaxial in-plane anisotropy was induced in CoNiFe films with an aligned magnetic field of 1000 Oe. The wafers are prepolarized in plating bath before any electrodeposition for 2 min with a small cathodic current (0.1 mA/cm^2) with no appreciable plating-taking place. The average thickness was obtained from nine measurement points distributed over entire wafer surface, A DekTek profilometer was used to take the step height as thickness.

The voltammetric measurements were performed in a 100 ml cell with Pt-rotating disc working electrode (A = 0.2 cm^2) or with EG&G flat sell (300 ml) onto which wafer could be clamped exposing 1 cm^2 of a film of sputtered Permalloy. A Pt counter electrode and saturated calomel electrode (SCE) as a reference electrode were used. In the experiments with RDE a Pine Instruments rotator was used. Potential–current curves were recorded using a Gamry Instrument PC3 potentiostat.

The *rms* roughness (average of four different points on the wafer) was obtained by AFM. The measured *rms* roughness of the seed layers was in the range of 0.4 – 0.6 nm. The surface roughness, R_g(L), is expressed in terms of the root mean square (*rms*) value, defined as

$$R_g(\mathrm{L}) = \sqrt{\sum_i^n (\bar{h} - h_i)^2 / n} \tag{1}$$

where n is the number of points measured across a surface $L \times L$, $\bar{h}$ is the average height, and h_i is the height of each point i. The *rms* roughness is calculated for varying sizes of the scanned area (0.01 μm^2 < $L \times L$ < 225 μm^2). Silicon nitride cantilevers were used.

RESULTS AND DISCUSSION

Electrochemistry.

Figure 1 shows current–potential curves for the CoNiFe plating bath in the absence or presence of organic additives using Permalloy as a cathode in quiescent solution. In the absence of organic additives the current increased gradually from the negative potential of

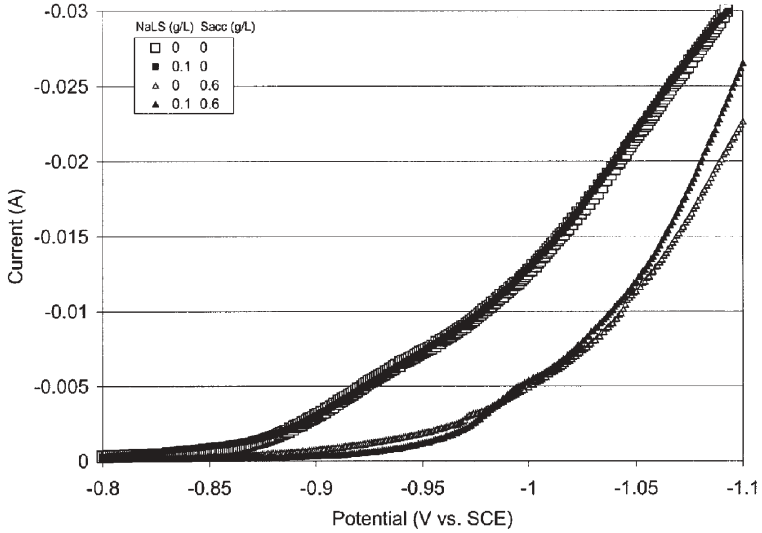

Fig. 1. Linear sweep voltammetric curves for CoNiFe deposition in 1 cm^2 stationary Permalloy electrode in plating bath (□) without additives, (■) with NaLS, (Δ) with Sacc, and (▲) with NaLS + Sacc; Sweep rate 1 mV/s.

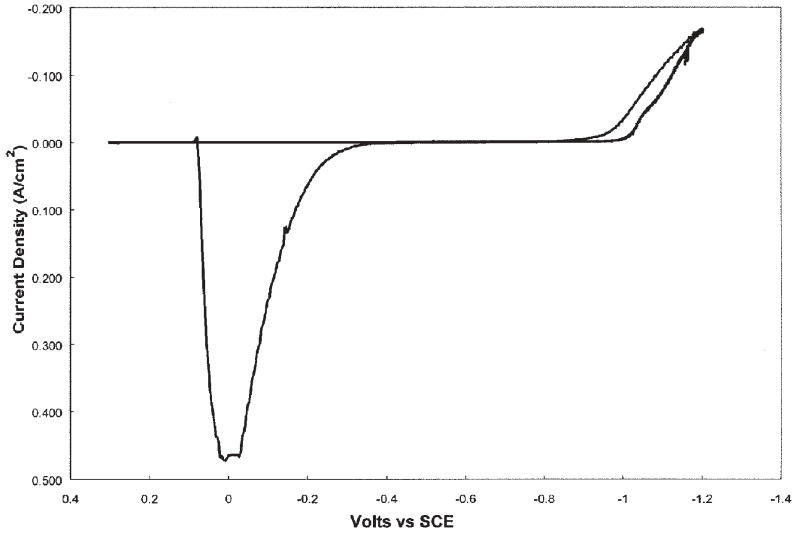

Fig. 2. Cyclic voltammogram of CoNiFe plating bath containing Sacc (0.6 g/l) and NaLS (0.1 g/l) at pH 2.8, Pt-RDE (0.2 cm^2), 200 rpm, v = 5 mV/s.

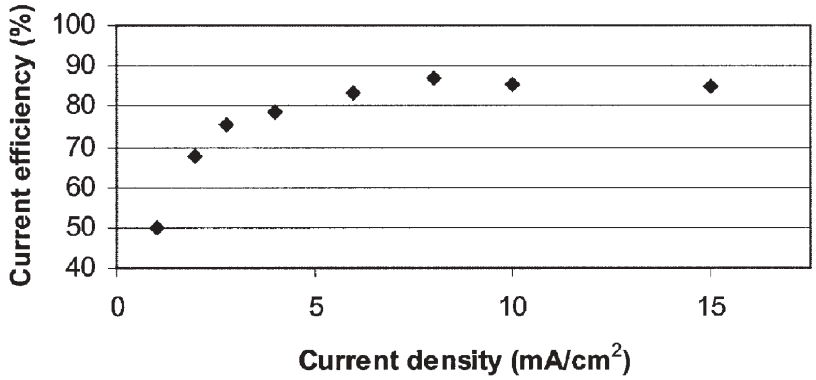

Fig. 3. Current efficiency *vs.* current density for electrodeposition of CoNiFe films.

–0.85 V *vs.* SCE due to the reduction of protons and metal ions. The polarization curve obtained in the presence of NaLS matches the curve obtained without organic additives. The addition of Sacc to the solution without additives or to the solution containing NaLS causes a significant shift of the reduction potential toward negative values presumably due to the surface coverage by adsorbed Sacc molecules.

Stripping cyclic voltammetry of the CoNiFe bath containing both additives (Sacc+NaLS) was carried out by using a rotating disc Pt-electrode in the potential range from 0.3 to –1.2 V *vs.* SCE (Fig. 2). Cathodic reduction of metal ions and protons starts around –0.95 V *vs.* SCE, while anodic oxidation and dissolution of CoNiFe film starts around –0.3 V *vs.* SCE.

In order to determine the current efficiency, the amount of charge for electrodeposition (Q_c) was kept constant (1.2 C) at different current densities. After electrodeposition the potential was set at 0.3 V *vs.* SCE and the amount of charge for dissolution (Q_a) was obtained by integrating the area under the anodic peak. The current efficiency defined as $Q_a/Q_c \times 100$ increased from 50 % at low current density to 85 % at higher current density (Fig. 3).

Morphology of CoNiFe films.

The morphology of the electrodeposit surface was imaged *ex situ* after CoNiFe electrodeposition using atomic force microscopy (AFM) operating in contact mode under ambient conditions. The morphology of CoNiFe films is influenced by the following variables: (*i*) thickness of deposit, (*ii*) presence of additives in solution, (*iii*) current density, (*iv*) temperature of plating bath, and (*v*) roughness of substrate.

Figure 4 shows three-dimensional AFM images obtained in the presence of NaLS+ Sacc additives at the current density of 3 mA/cm^2 as a function of thickness. The pictures were taken at same vertical scale (30 nm/div) and for scanning surface 10 ×10 μm^2. The thin (0.21 μm) film shows smooth granular structure. The height of hills formed increases as well as *rms* roughness with the increase of deposit thickness. The thick film (1.82 μm) shows smaller peak density which suggest that peaks overlap during the growth phase.

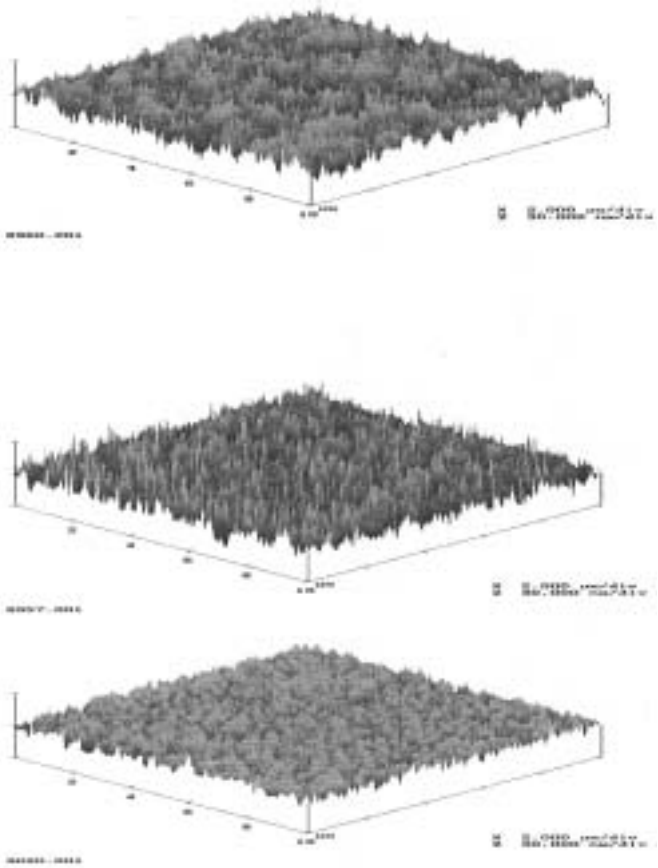

Fig. 4. AMF images of CoNiFe surfaces produced with different thickness in the presence of NaLS + Sacc. Bottom 0.21 μm (R_g = 4.55 nm), Middle 0.89 μm (R_g = 5.71 nm), Top 1.82 μm (R_g = 6.32 nm).

Figure 5 shows a sequence of AFM images with comparable thickness (1.5 ± 0.05 μm) of CoNiFe films obtained from solutions containing different organic additives. The pictures were taken at the same vertical scale (250 nm/div) and for two scanning surfaces, *i.e.*, 10 × 10 and 1 × 1 μm, respectively.

The surface grown from NaLS is very rough (R_g = 62.36 nm) with threedimensional islands (Fig. 5, Top). Large nuclei would be expected to form when surface diffusion of adatoms on the deposited surface was relatively unhindered. Notably, the voltammetry of the NaLS solution is the same as a solution without any additives (Fig. 1). The AFM image of surface grown without additives, not shown here, is very similar to the image in Fig. 4 Top. On the other hand, the surfaces grown from Sacc solution with R_g = 5.61 nm and NaLS + Sacc solution with R_g = 5.95 nm are smooth. Inspection of surfaces produced from the Sacc solution using SEM (Fig. 6) revealed the presence of pits that are due to surface bubbles from hydrogen evolution. Similar pits (bubble tracks) were found on the nickel electrodeposits produced from a Watt's solution.[19]

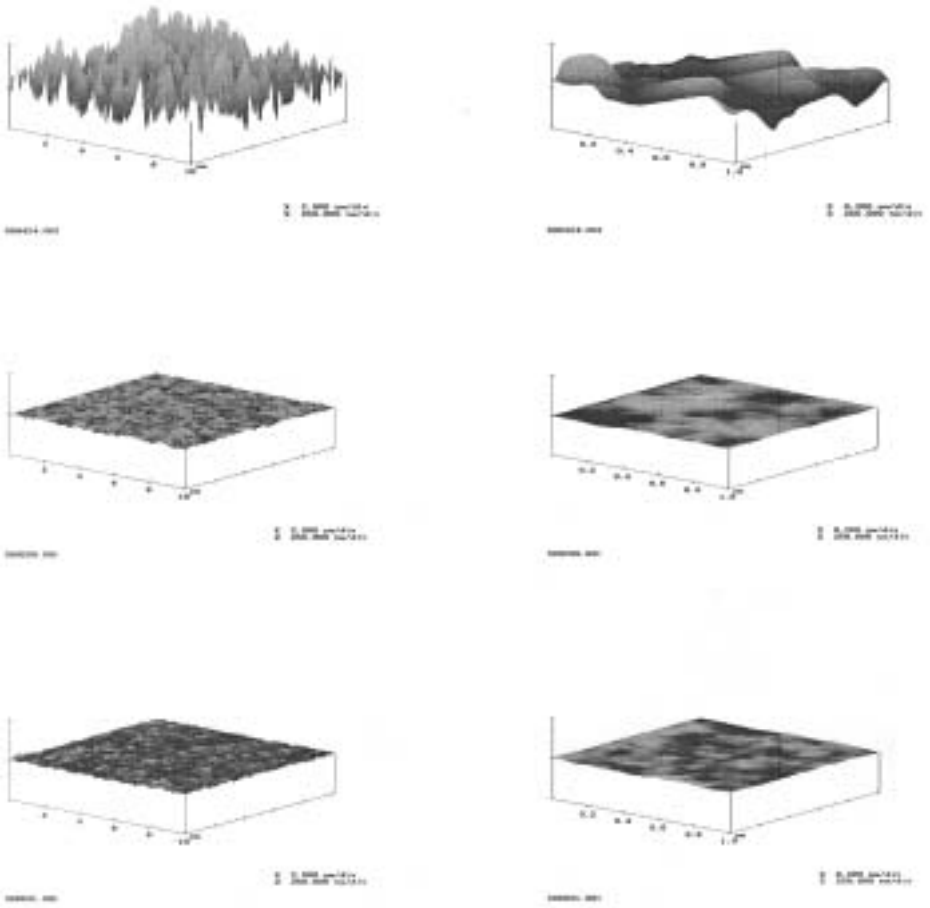

Fig. 5. AMF images of CoNiFe surfaces produced from three solutions: Bottom (Sacc), Middle (NaLS + Sacc), Top (NaLS).

During the CoNiFe electrodeposition part of the current is consumed by hydrogen evolution. The hydrogen can be attached as an adsorbed molecule at the electrode surface during the electrodeposition. The rate of electrodeposition is inhibited at the sites of hydrogen attachment, which results in the observed pits on the plated surface. However, SEM images of CoNiFe surfaces produced in the presence of both additives (Sacc + NaLS) did not show the characteristic pits. These experiments suggest a possible role of NaLS used in CoNiFe and NiFe plating baths. The NaLS surfactant changes the interfacial tension and can help blocking non-polar species like hydrogen bubbles leave the surface.

In order to examine the influence of current density on roughness of CoNiFe films, several films with the thickness of 0.7 ± 0.05 μm were electrodeposited. The *rms* roughness, R_g, increases with the increase of current density (Fig. 7). Notably, the contribution of the proton discharge reaction to the total current decreases from 1 to 15 mA/cm^2 (Fig. 3). It is assumed that formation of hydrogen bubbles at peaks should be enhanced. Therefore,

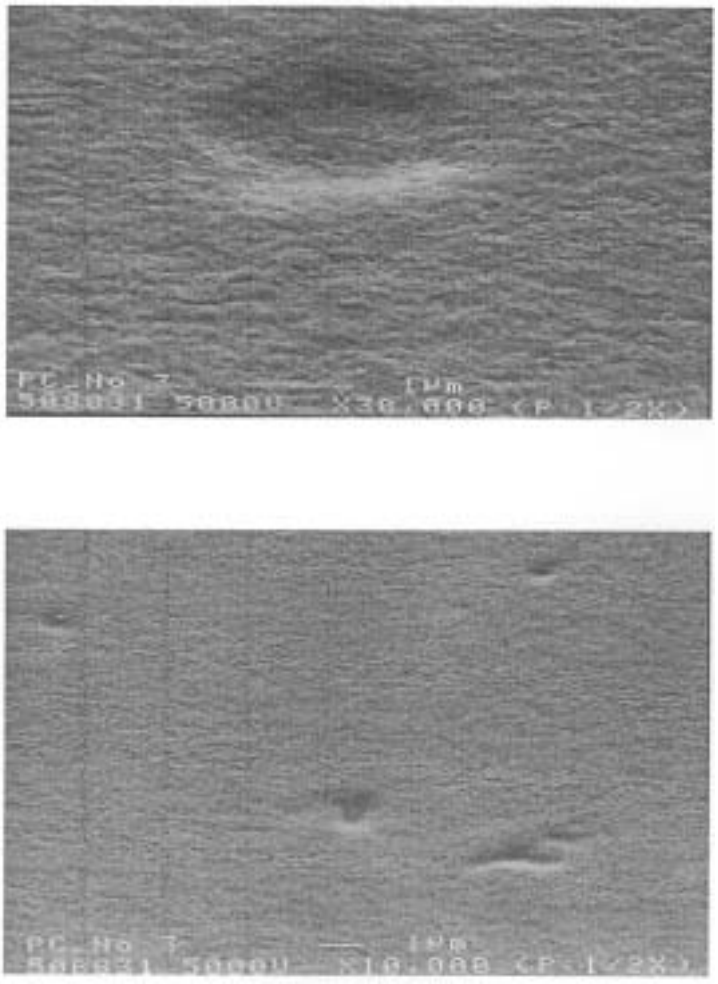

Fig. 6. SEM images of pits on a CoNiFe surface produced from Sacc containing solution.

the discharge of metal ions is relatively hindered at the peaks and enhanced in the valleys, which result with a smoother surface.

The increase of temperature of plating solution from 23 ºC to 40 ºC exhibits a smoothening effect on CoNiFe films (Fig. 8). The presence of Sacc in plating solution is a dominating parameter, which effects roughness. The increase of temperature probably effects the adsorption/desorption kinetics of Sacc giving rise to smaller roughness.

Most of the experiments were performed with a wafers having a Permalloy (1.0T NiFe) seed layer. Importantly, the measured *rms* roughness of 1000 Å of 1.0T NiFe seed layer varied from 0.4 to 0.6 nm. In order to examine the influence of the substrate roughness we have used wafers with HMM CoFe seed layer which had *rms* roughness between 2–3 nm. The roughness of electrodeposited CoNiFe films is influenced by the roughness of substrates which is illustrated in Fig. 9.

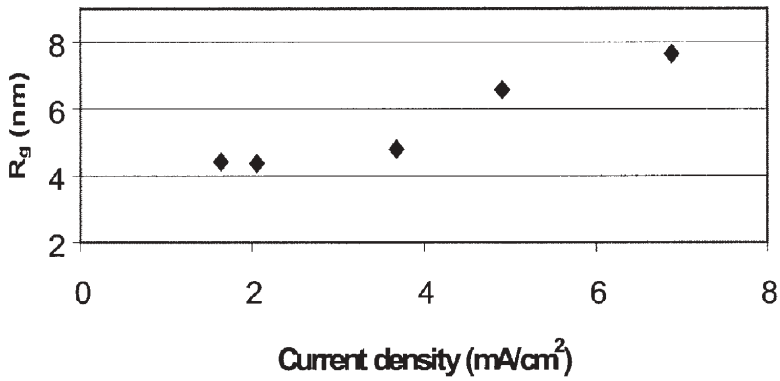

Fig. 7. Effect of current density on *rms* roughness, R_g, obtained in CoNiFe plating solution containing NaLS + Sacc additives.

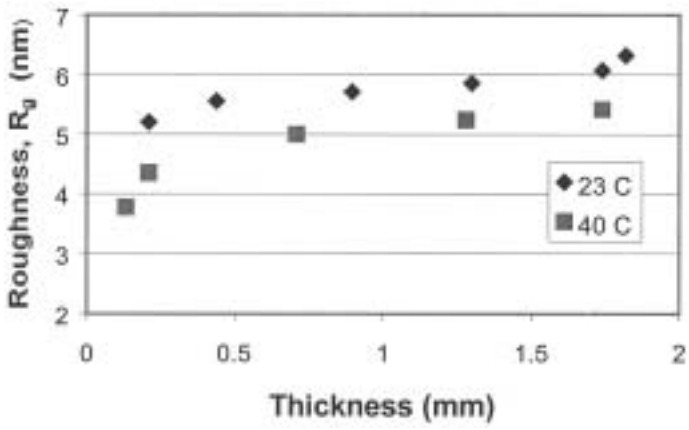

Fig. 8. Effect of temperature on *rms* roughness, R_g, obtained in CoNiFe plating solution containing NaLS + Sacc additives.

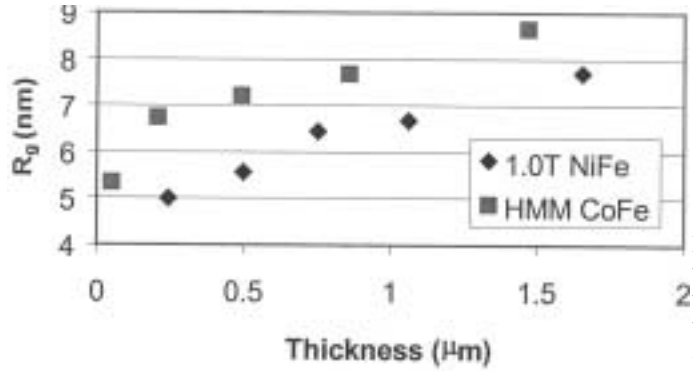

Fig. 9. Effect different substrates on *rms* roughness, R_g, obtained in CoNiFe plating solution containing NaLS + Sacc additives.

Scaling analysis.

The electrodeposition of metals from an additive-free plating bath and near the mass-transfer limited current is related to the development of an unstable interface originating from the enhanced electrodeposition at the protrusions.[20] Roughness development is amplified during deposition because the current is higher on protrusions than on the surrounding surfaces (valleys). Theoretical studies treat the growth of rough and fractal sur-

faces built up during deposition which satisfies the Laplace equation.[21] The presence of small amounts of adsorption additives in the plating bath results generally with smooth surfaces. At slow growth rates, the growth is controlled by local and non-local effects[22] such as diffusion of metal ion, heterogeneous rate of electron transfer, surface diffusion of adatoms, and adsorption/desorption kinetics of additives.

In general, the kinetics of phase growth can be studied by applying the dynamic scaling theory[21] to surface properties. Films grown under nonequilibrium conditions are expected to develop self-affine surfaces.[22] A self-affine surface is one that changes morphology when scale change is made in all directions. All rough surfaces exhibit perpendicular fluctuations that are characterized by *rms* roughness, which depends on the length scale of observation. The dynamic scaling theory predicts that *rms* roughness, σ, scales with time (or thickness) t, and the length L, sampled as:[22]

$$\sigma(L,t) = L^{\alpha} f(t/L^{\alpha/\beta}) \tag{2}$$

where $\sigma(L) \propto L^{\alpha}$ for $t/L^{\alpha/\beta} \rightarrow \infty$ and $\sigma(t) \propto t^{\beta}$ for $t/L^{\alpha/\beta} \rightarrow 0$. The parameter α is the roughness exponent and parameter β is the growth exponent. The roughness exponent, α, characterizes the roughness of saturated interface and growth exponenet, β, characterizes the time-dependent dynamics of roughening surface. The roughness, $\sigma(L)$, does not scale indefinitely but reaches a saturation value σ_{sat}. The characteristic length above which σ becomes equal to σ_{sat} is known as the critical scaling length L_c. Implicit in Eq. (2) is the relation of the critical scaling length, L_c, with time (or thickness), t,

$$L_c = t^{1/z} \tag{3}$$

$$z = \alpha/\beta \tag{4}$$

where z is the dynamic scaling exponent.

Figure 10 shows the typical experimental relationship between *rms* roughness, R_g, and L for CoNiFe films of different thickness, (0.11, 0.31, and 1.76 μm, respectively) prepared from plating solution containing NaLS+Sacc additives. For each thickness, the curve consists of two regimes separated by the critical length, L_c, *i.e.*, the scale-dependent region and the saturation region.

Figure 11 shows the experimental relationship of the variation of the *rms* roughness, R_g, with the length scale in the scale-dependent region, *i.e.*, for $L < L_c$. The roughness exponent, α, is determined by linear regression analysis of the log–log slope of the *rms* variation with the sample size for three plating solution, *i.e.*, NaLS, Sacc, and Sacc+NaLS (see Table I).

The growth exponent, β, was calculated from log–log plot of R_g measured at saturation roughness (L = 15 μm) at thickness, t, for different plating solutions (Fig. 12). Values of the experimentally determined scaling analysis parameters (α and β) are collected in Table I.

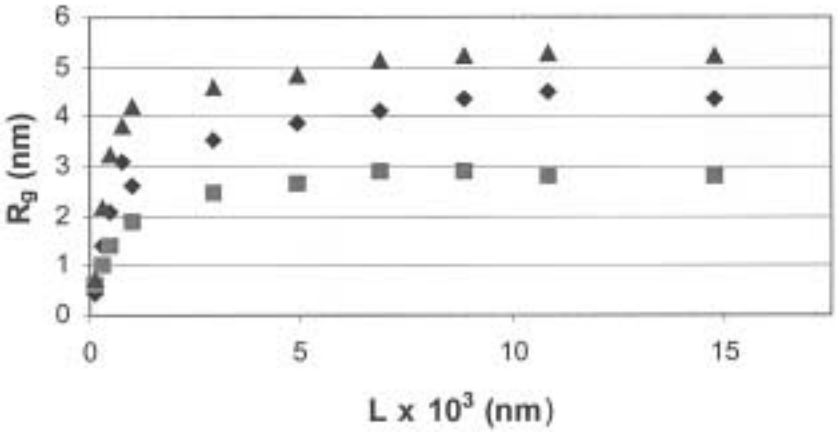

Fig. 10. Relationship between R_g and L for CoNiFe films of different thickness: (■) 0.11 μm, (◆) 0.31 μm, (▲) 1.76 μm.

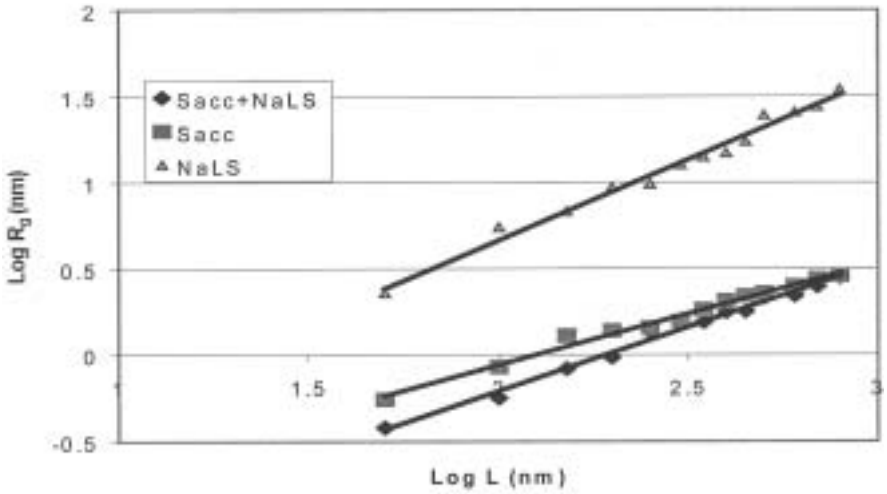

Fig. 11. log R_g *vs.* log L of CoNiFe electrodeposits produced from plating bath with three different additives and thickness of $t = 1.3 \pm 0.05$ μm.

TABLE I. Experimentally determined scaling analysis parameters

Solution	α	β
NaLS	0.93 ± 0.06	0.63 ± 0.05
NaLS + Sacc	0.73 ± 0.03	0.135 ± 0.02
Sacc	0.59 ± 0.02	0.126 ± 0.01

The values of α and β can be compared to those derived theoretically from atomistic and continuum models for interface evolution.[21] The values of the scaling exponents for three dimensional space (3D) are presented in Table II.

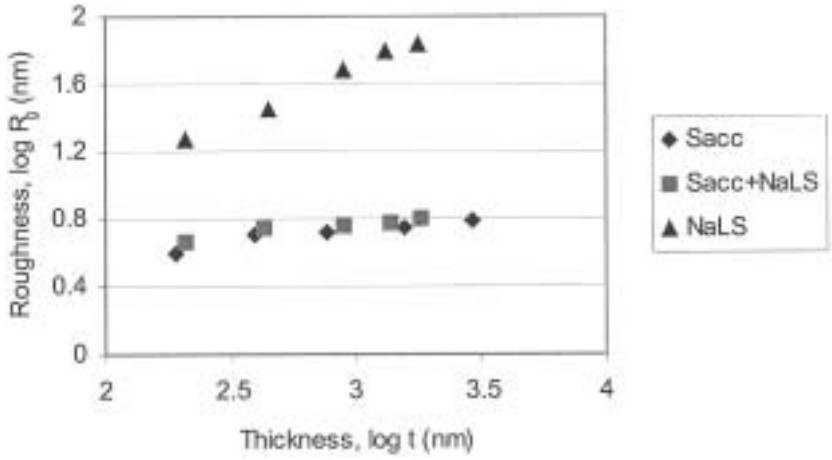

Fig. 12. log R_g *vs.* log L of CoNiFe electrodeposits produced from plating bath with three different additives and $L = 15 \times 15$ μm^2.

TABLE II. The scaling parameters predicted by various models

Model*	α	β	Comment	Ref.
RD	0	0.5	Deposition without latheral growth	21
BD – surface relaxation	0.36	0.22	Deposition with latheral growth	23,24
EW	0	0	Erosion of protrusions and filling of recesses	25
KPZ	0.39	0.25	Deposition with latheral growth through diffusion of ad-atoms	26
WV	1.0	0.25	Surface diffusion	27
WV + step flow	0.66	0.2	Surface diffusion and step growth	28

*RD – Random distribution, BD – Balistic deposition, EW – Edwards Wilkinson, KPZ – Kadar, Parisi, Zhang, WV – Wolf, Vilian

During the last few years, the dynamic scaling analysis has been applied to study copper electrodeposition with and without organic additives present in the plating solution. Depending on experimental conditions, the copper electrodeposits without additives exihibited a wide range of α ($0.33 \leq \alpha \leq 0.91$) and β ($0.11 \leq \beta \leq 0.63$) values. In the presence of additives, the values of α ($0.46 \leq \alpha \leq 0.86$) and β ($0.23 \leq \beta \leq 0.63$) are generally lower but exihibit also a wide range values.[14–18,29,30]

Our results showed the value of α is such that $0 < \alpha < 1$ indicating a self-afine surfaces obtained by electrodeposition in the presence of different additives. The electrodeposition of CoNiFe films from NaLS solution produced rough surfaces, while plating from Sacc or Sacc+NaLS solution gave a smooth surfaces. These observations are in accordance with the recent results obtained using the same additive during pulse deposition of CuCo alloys.[31] For NaLS solution, the value of $\alpha = 0.93 \pm 0.06$ appears to be consistent with WV growth models[27] incorporating unhindered surface diffusion of atoms. The high value of β

$= 0.63 \pm 0.05$ exceeds the value expected from VW model (see Table II). The value $\beta > 0.5$ is characteristic of unstable growth where local growth effects complete with the nonlocal Laplacian effects.[16] The activity of the metal, and hence the deposition potential, is higher for a curved surface than for a flat one, an effect referred as capillarity.[32] Therefore, when protrusions are formed they can grow faster than valleys which results in unstable growth.

In Sacc and NaLS + Sacc containing solutions the values of both exponents, *i.e.*, α and β, are smaller than with the NaLS solution (see Table I) and the evolution of the smooth surface is mediated by adsorbed Sacc molecules at the surface. The obtained values of the scaling parameters for NaLS + Sacc and Sacc solutions (Table I) are consistent with parameters obtained from models for the "WV + step flow" growth mechanism.[28] This mechanism involves a lateral mass transport process by surface diffusion of ad-atoms to the nearest kink sites. It is well known that organic molecules adsorbed at the metal/electrolyte interface, reduce the surface diffusion coefficient of metal ad-atoms and accordingly, the diffusion length.[31] We assume that the Sacc additive is preferentially adsorbed at protrusions on the CoNiFe surface. The higher additive molecule coverage at the protrusions slows down the rate of charge transfer reaction from metal ions but increases the rate of electrodeposition in the valleys where the degree of surface coverage by additive is lower than at protrusions. Once the leveling of the surface is produced there is no longer a variation in the local potential distribution and the adsorbate layer attains a more uniform distribution.

ИЗВОД

ПРОМЕНА ХРАПАВОСТИ ПОВРШИНЕ CoNiFe ФИЛМОВА ДОБИВЕНИХ ЕЛЕКТРОДЕПОЗИЦИЈОМ У ПРИСУСТВУ ОРГАНСКИХ АДИТИВА

ИБРО ТАБАКОВИЋ и STEVE REIMER

Seagate Technology, One Disc Drive, Bloomington, MN 55435, USA

Изучаван је утицај три адитива, натријум-лаурилсулфата (NaLS), сахарина (Sacc) и NaLS + Sacc на храпавост површине CoNiFe филмова добивених електродепозицијом. Испитивање ових филмова AMF микроскопијом указује на велику храпавост површине филмова добивених у присуству NaLS. Улога NaLS сурфактанта је да мења површински напон и помаже уклањању мехурића водоника са површине. У растворима који садрже Sacc стварање глатких површина је контролисано адсорбованим молекулима сахарина на граници фаза. Динамичка анализа је употребљена за увид у кинетику развоја површине. Резултати су показали да храпавост површине зависи такође од густине струје, храпавости супстрата и температуре електролита.

(Примљено 10. септембра 2002)

REFERENCES

1. P. C. Andricacos, N. Robertson, *IBM J. Res. Dev.* **42** (1998) 672
2. T. Osaka, M. Takai, K. Hayashi, K. Okashi, M. Saito, K. Yamada, *Nature* **292** (1998) 796
3. I. Tabaković, S. Riemer, V. Inturi, P. Jallen, A. Thayer, *J. Electrochem. Soc.* **147** (2000) 219
4. X. Liu, P. Evans, G. Zangari, *J. Appl. Phys.* **87** (2000) 5410

5. I. Tabaković, V. Inturi, S. Riemer, *J. Electrochem. Soc.* **149** (2002) C18
6. K. Liy, J. W. Chang, L. T. Romankiw, D. A. Herman, in *Magnetic Materials, Processes and Devices*, L. T. Romankiw, D. A. Herman, Eds., The Electrochemical Society Proceedings Series, PY 95-18, Pennington, NJ, 1990, p. 626
7. Y. Nakamura, N. Kaneko, M. Watanabe, H. Nezu, *J. Appl. Electrochem.* **24** (1994) 227
8. J. Macheras, D. Vouros, C. Kollia, N. Spyrellis, *Trans. IMF* **74** (1994) 55
9. C.–Z. Gao, Y–I. Lu, H. T. Wang, S.–B. Yue, *Trans. IMF* **77** (1999) 192
10. V. Darrort, M. Troyon, J. Ebothe, C. Bissieux, C. Nicollin, *Thin. Solid Films.* **265** (1995) 52
11. G. Palasantzas, J. Krim, *Phys. Rev. Lett.* **26** (1994) 3564
12. C. Eisenmenger-Sittner, A. Bergauer, H. Baugert, W. Baure, *J. Appl. Phys.* **78** (1995) 4899
13. L–H. Tang, T. Nattermann, *Phys. Rev. Lett.* **66** (1991) 2899
14. W. U. Schmidt, R. C. Alkire, A. A. Gewirth, *J. Electrochem. Soc.* **143** (1996) 3122
15. M. Cerisier, K. Attenborough, J. Fransear, C. Van Haesendonck, J. –P. Celis, *J. Electrochem. Soc.* **146** (1999) 2156
16. S. Mendez, G. Andreasen, P. Schilardi, M. Figueroa, L. Vasquez, R. S. Salvarezza, A. J. Arvia, *Langmuir* **14** (1998) 2515
17. G. L. M. K. S. Kahanda, X. –G. Zou, R. Farrell, P. –Z. Wong, *Phys. Rev. Lett.* **68** (1992) 3741
18. H. Iwasaki, T. Yoshinobu, *Phys. Rev. Lett.* **48** (1993) 8282
19. O. Devos, A. Olivier, J. P. Chaport, O. Aaboubird, G. Mauriu, *J. Electrochem. Soc.* **145** (1998) 401
20. D. P. Barkey, R. H. Muller, C. W. Tobias, *J. Electrochem. Soc.* **136** (1989) 2199
21. E. Stanly, A. Barabasi in *Fractal Concepts in Surface Growth*, Cambridge University Press, New York, 1994
22. A. Iwamoto, T. Yoshinobu, H. Iwasaki, *Phys. Rev. Lett.* **72** (1994) 4025 and the references threin
23. P. Meakin, R. Jullien, *J. Physique* **48** (1987) 1651
24. R. Jullien, P. Meakin, *Europhys. Lett.* **4** (1987) 1385
25. S. F. Edwards, D. R. Wilkinson, *Proc. Royal Soc., London A.* **381** (1982) 17
26. M. Kardar, G. Parisi, Y. –C. Zhang, *Phys. Rev. Lett.* **56** (1986) 889
27. D. E. Wolf, J. Vilian, *Europhys. Lett.* **13** (1990) 389
28. J. Vilian, *J. Phys*, *I*, **1** (1991) 19
29. T. Y. B. Leung, M. Kang, B. F. Corry, A. W. Gewirth, *J. Electrochem. Soc.* **147** (2000) 3326
30. T. F. Otero, J. L. Rodriguez-Jimanez, H. Martin, P. Carro, S. M. Krijer, A. Hernandez-Creus, *J. Electrochem. Soc.* **147** (2002) 4546
31. J. J. Kelly, P. E. Bradley, D. Landolt, *J. Electrochem. Soc.* **147** (2000) 2975
32. A. R. Despić, K. I. Popov, in *Modern Aspects of Electrochemistry*, J. O'M Bockirs, B. E. Conway Eds., Butterworths, New York, 1972, Vol. 7, Ch. 4, p. 199.